ChemPubSoc Europe

DOI: 10.1002/chem.201702335

CHEMISTRY A European Journal Communication

Radiochemistry |*Hot Paper*|

Dual-Nuclide Radiopharmaceuticals for Positron Emission Tomography Based Dosimetry in Radiotherapy

Alexander Wurzer,[a] Christof Seidl,[b, c] Alfred Morgenstern,[d] Frank Bruchertseifer,[d] Markus Schwaiger,[b] Hans-Jürgen Wester,[a] and Johannes Notni*[a]

Abstract: Improvement of the accuracy of dosimetry in radionuclide therapy has the potential to increase patient safety and therapeutic outcomes. Although positron emission tomography (PET) is ideally suited for acquisition of dosimetric data because PET is inherently quantitative and offers high sensitivity and spatial resolution, it is not directly applicable for this purpose because common therapeutic radionuclides lack the necessary positron emission. This work reports on the synthesis of dual-nuclide labeled radiopharmaceuticals with therapeutic and PET functionality, which are based on common and widely available metal radionuclides. Dual-chelator conjugates, featuring interlinked cyclen- and triazacyclononane-based polyphosphinates DOTPI and TRAP, allow for strictly regioselective complexation of therapeutic (e.g., ^{177}Lu, ^{90}Y, or ^{213}Bi) and PET (e.g., ^{68}Ga) radiometals in the same molecular framework by exploiting the orthogonal metal ion selectivity of these chelators (DOTPI: large cations, such as lanthanide(III) ions; TRAP: small trivalent ions, such as Ga^{III}). Such DOTPI–TRAP conjugates were decorated with 3 Gly-urea-Lys (KuE) motifs for targeting prostate-specific membrane antigen (PSMA), employing Cu-catalyzed (CuAAC) as well as strain-promoted (SPAAC) click chemistry. These were labeled with ^{177}Lu or ^{213}Bi and ^{68}Ga and used for in vivo imaging of LNCaP (human prostate carcinoma) tumor xenografts in SCID mice by PET, thus proving practical applicability of the concept.

Radionuclide therapy[1] (also termed molecular radiotherapy) is the internal application of radionuclides or radiolabeled compounds for therapeutic purposes, above all, for treatment of cancer. In this context, the term "dosimetry" refers to the assessment of absorbed radiation energy per tissue volume, derived from spatially resolved radioactivity distribution data over time. Hence, the averagely delivered tissue doses of a radiotherapeutic are governed by many factors, such as the decay characteristics of the radionuclide used, the radiopharmaceutical's metabolic stability, excretion kinetics and route, its target affinity and specificity, and its specific uptake and retention in targeted as well as in non-targeted organs and tissues. However, individual doses may vary[2] because uptake of a radiopharmaceutical in tumors and in organs and tissues at risk is also dependent on methodological and patient-specific factors, such as variations of the administered mass dose of the radiopharmaceutical,[3–7] cumulative tumor mass,[8] tumor perfusion,[9] expression density of the target (e.g., of a surface receptor) on tumor cells,[10,11] individual and gender-dependent metabolic rates, body weight or altered excretion kinetics (e.g., renal impairment). A personalized dosimetry is thus a necessary prerequisite to assess such interindividual variations in clinical trials, in order to optimize treatment protocols, to maximize tumor doses, to improve the individual therapeutic outcome, and to increase patient safety.[2,12]

For targeted radionuclide therapy, specific receptor ligands or enzyme inhibitors (e.g., oligopeptides or peptoids) are usually equipped with suitable chelators[13] (mostly based on the structural motif DOTA)[14] and labeled with radiometal ions, such as the β^--emitters ^{177}Lu^{III} or ^{90}Y^{III}, or, less frequently, α-emitters like ^{213}Bi^{III} or ^{225}Ac^{III}.[15] Dosimetry usually relies on planar scintigraphy or single-photon emission computed tomography (SPECT),[16,17] exploiting additional γ-emissions of these nuclides, or by "spiking" with a matched γ-emitter (e.g., partially replacing ^{90}Y^{III}, which has no photon emission, with ^{111}In^{III}).[18] In this context, it has been pointed out earlier that positron emission tomography (PET) is particularly attractive for acquiring dosimetric data, because PET is very sensitive and capable of quickly delivering quantitative spatial distribution

[a] *A. Wurzer, Prof. Dr. H.-J. Wester, Dr. J. Notni*
Pharmaceutical Radiochemistry, Technische Universität München
Walther-Meißner-Strasse 3, 85748 Garching (Germany)
E-mail: johannes.notni@tum.de
Homepage: http://www.prc.ch.tum.de

[b] *Dr. C. Seidl, Prof. Dr. M. Schwaiger*
Department of Nuclear Medicine
Technische Universität München (Germany)

[c] *Dr. C. Seidl*
Department of Obstetrics and Gynecology
Technische Universität München (Germany)

[d] *Dr. A. Morgenstern, Dr. F. Bruchertseifer*
European Commission, Joint Research Centre, Directorate for Nuclear Safety and Security, Karlsruhe (Germany)

Supporting information and the ORCID identification number for the author of this article can be found under https://doi.org/10.1002/chem.201702335.

data with high resolution, and is thus, in principle, superior to SPECT and scintigraphy.[19]

However, virtually all therapeutic radiometals are lacking the necessary β^+-emissions. Hence, spiking with a β^+-emitting isotope of the same element has been recommended, for example, a partial replacement of ^{90}Y with ^{86}Y,[20] which enabled improved dosimetry compared to ^{111}In-SPECT.[21,22] Apart from the fact that this approach is not applicable to elements devoid of β^+-emitting isotopes, such as Bi, it suffers from insufficient availability of all relevant surrogate PET nuclides. Furthermore, many of them exhibit unfavorable decay properties, such as additional high-energy gamma lines, which challenge PET quantitation by false coincidences due to scatter photons and cause high radiation doses to operating and nursing personnel.

Alternatively, the therapeutic metal ion can be exchanged with a chemically different β^+-nuclide, such as ^{68}Ga^{III}.[23–25] Indeed, pre-therapeutic PET scans obtained with ^{68}Ga-DOTA-peptides are frequently employed for therapy decisions,[3,4,26] whereas their value for dosimetry is limited due to mismatching half-lives (68 min for ^{68}Ga vs. several days for ^{90}Y or ^{177}Lu). Furthermore, this approach inherently lacks precision because ^{68}Ga^{III}- and other radiometalated DOTA-conjugates frequently exhibit different target-to-organ ratios[27,28] due to deviations in pharmacodynamics, which in turn result from different polarities owing to mismatched coordination modes (Ga^{III}-DOTA: hexadentate, zwitterionic; Ln^{III}-, Sc^{III}-, Y^{III}-, Bi^{III}-DOTA: nona- or octadentate, uncharged).[13]

To overcome these limitations, we herein propose radiopharmaceuticals bearing both a therapeutic and a PET-radiometal at defined locations. We primarily focused on the emerging therapeutic α-emitter ^{213}Bi,[15] because in view of its short half-life ($T_{1/2}$ = 46 min), accuracy of dosimetry particularly benefits from the high temporal resolution achievable by dynamic PET. ^{68}Ga^{III} ($T_{1/2}$ = 68 min) ideally complements ^{213}Bi in terms of half-life and accessibility as both are obtained from commercially available radionuclide generators (small chromatographic benchtop devices acting as regenerative nuclide sources).[15,23–25]

To achieve regiospecific complexation of Ga^{III} and Bi^{III}, we decided to exploit the complementary metal ion selectivity of the homologous phosphinate chelators DOTPI[29] (large trivalent cations) and TRAP[30] (small trivalent cations, particularly Ga^{III}),[31–33] which were linked through their N-pendant arms (Scheme 1). First, DOTPI was equipped with four terminal azide groups. Employing CuAAC or SPAAC, DOTPI(azide)$_4$ was further decorated with three copies of PA-Ahx-KuE or DBCO-Ahx-KuE, wherein KuE (glutamic acid-urea-lysine) is an inhibitor motif for prostate-specific membrane antigen (PSMA, EC 3.4.17.21, synonyms: glutamate carboxypeptidase II, NAALADase;[34] a membrane-bound zinc hydrolase that is overexpressed by malignant human prostate cancers). Subsequent conjugation of TRAP was done by CuAAC coupling of TRAP-monopropargylamide[35] followed by competitive Cu-demetalation,[36,37] leading to the PSMA inhibitor trimers DOTPI(PA-Ahx-KuE)$_3$(TRAP) (**1**) and DOTPI(DBCO-Ahx-KuE)$_3$(TRAP) (**2**) (Scheme 1; isolated yields were 19 and 10%, respectively, based on DOTPI(azide)$_4$).

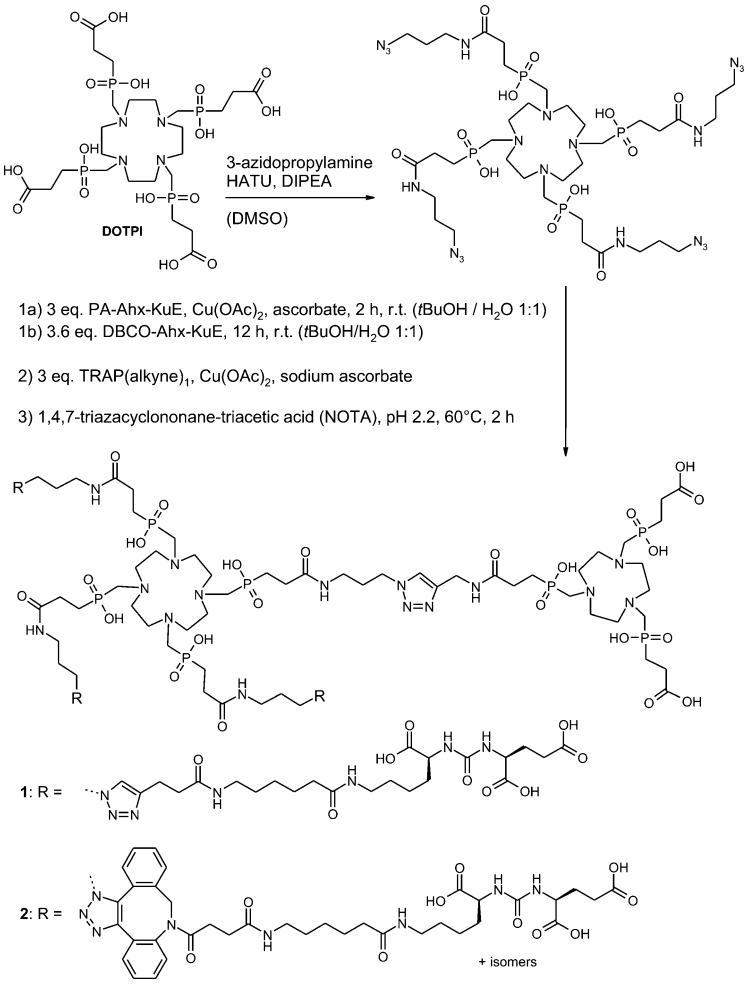

Scheme 1. Synthesis of trimeric PSMA inhibitors featuring the DOTPI-TRAP interlinked chelator system for regioselective complexation of different radiometal ions by means of azide–alkyne cycloaddition, both the Cu^I-mediated (CuAAC, step 1a) as well as the DBCO-driven, Cu-free variant (SPAAC, step 1b).

To demonstrate the feasibility of the concept not only for Bi^{III} but for radiolanthanides in general, precursors for radiometal complexation were prepared from **1** and **2** by complexation of DOTPI with M^{III} (M = Lu, Bi) or of TRAP with Ga^{III} according to Scheme 2. In either case, both chelator cages were initially saturated using an excess of the respective metal ion. Subsequently, selective removal of M^{III} from TRAP and Ga^{III} from DOTPI, respectively, was achieved by exploiting the substantially different coordination behavior of the complexes. Because neither the [M^{III}(TRAP)][38,39] nor the [Ga^{III}(DOTPI)][29] system is particularly stable or kinetically inert, removal of metal ions from these chelates is feasible by means of transchelation with (aq.) Na$_3$DTPA or Na$_2$EDTA, respectively, under which conditions the respective other complexes, [M^{III}(DOTPI)] and [Ga^{III}(TRAP)], remain intact because of their high kinetic inertness. Starting from these complexes, heteroleptic chelates [Ga^{III}][Bi^{III}]-**1** and

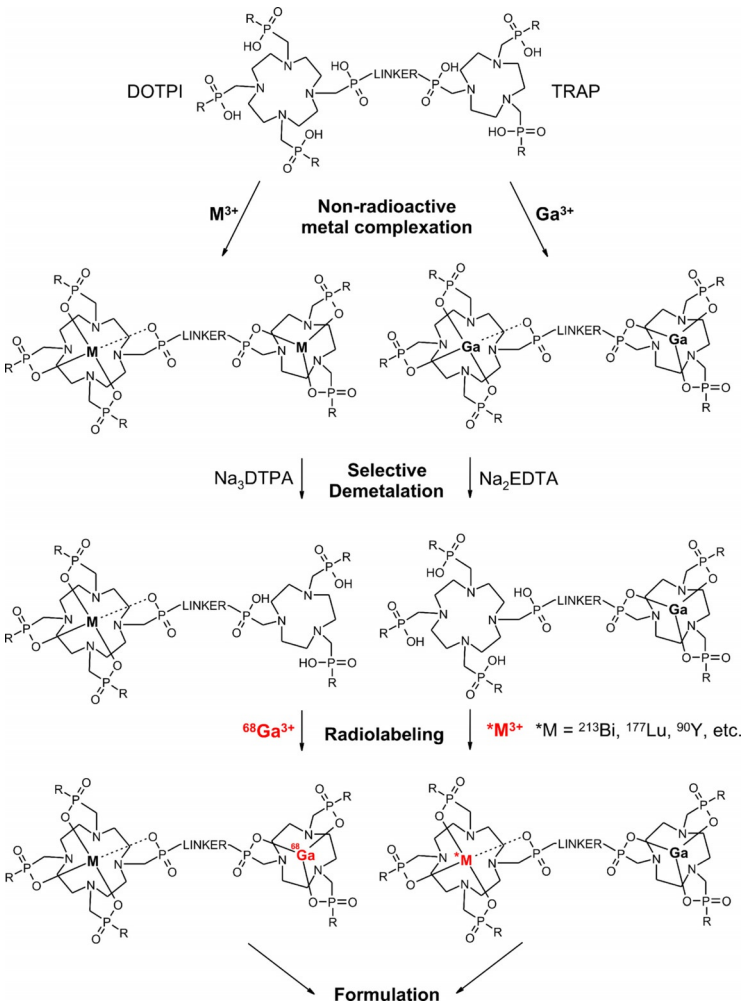

Scheme 2. Principle of preparation of dual-nuclide radiopharmaceuticals based on DOTPI–TRAP conjugates (simplified scheme without complex charges and M^{k+}–N coordination bonds). Precursors for labeling with therapeutic nuclides $*M^{III}$, for example, radiolanthanides, Bi-, and Y-isotopes, are obtained by saturation of the TRAP cage with inactive Ga^{III}. Likewise, precursors for labeling with ^{68}Ga are produced by selective complexation of the inactive M^{III} isotopes. The generic "R" refers to any possible substituent, not implicating similarity of any residues involved.

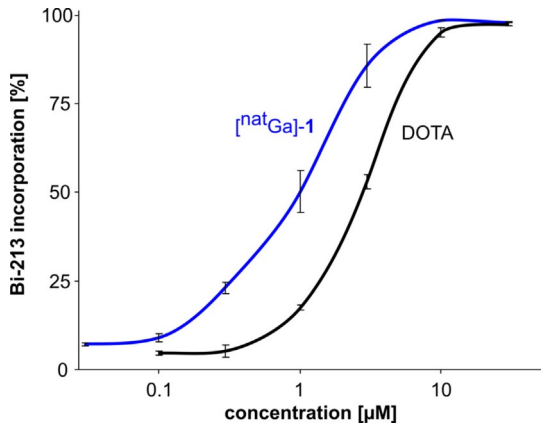

Figure 1. Incorporation of ^{213}Bi (5 min, 95 °C, pH 5.3) as functions of concentration, determined for [Ga]-**1**. The corresponding curve for DOTA shows that Bi^{III} complexation by the DOTPI chelator is more efficient. DOTA = 1,4,7,10-tetraazacyclododecane-1,4,7,10-tetraacetic acid.

$[Ga^{III}][Lu^{II}]$-**2** were obtained by complexation of the respective nonradioactive metals (see the Supporting Information).

Radiolabeling can be done straightforwardly according to standard protocols (complexation of $*M^{III}$ or $^{68}Ga^{III}$ in aqueous solution buffered to pH 5–7 or pH 3, respectively, at elevated temperature). Interestingly, we noted that incorporation of $^{213}Bi^{III}$ by [natGa]-**1** using the pH-adjusted eluate of a $^{225}Ac/^{213}Bi$ generator ($[^{213}BiI_4]^-$ and $[^{213}BiI_5]^{2-}$ in 3 M (aq.) NH_4OAc, pH 5.3, see the Supporting Information) required lower concentrations of [natGa]-**1** as compared to DOTA, highlighting a higher ^{213}Bi labeling efficiency of the DOTPI chelator system (Figure 1).

For proof-of-concept PET imaging, [natBi]-**1** and [natLu]-**2** were labeled with ^{68}Ga applying a standard automated protocol[40] and administered to SCID mice bearing LNCaP (human prostate carcinoma) xenografts (Figure 2). For [natBi][^{68}Ga]-**1**, a slightly lower uptake in tumor and background, a markedly lower activity concentration in the kidneys, and a slightly higher uptake in the salivary glands was observed compared to [natLu][^{68}Ga]-**2** (see Table 1). The DBCO-moieties of compound **2** effect a slightly lower degree of hydrophilicity compared to **1** (-3.8 ± 0.1 vs. -4.4 ± 0.1, respectively). Because of the multimer effect, PSMA affinities (expressed as IC_{50}, determined in displacement assays on LNCaP cells) of compounds **1** and **2** are high (2.5 ± 0.2 and 2.8 ± 0.3 nM, respectively) and exceed those of clinically applied PSMA ligands.[41,42]

In conclusion, we have shown that interlinked chelators with orthogonal kinetic inertness profiles provide facile access to pairs of ^{68}Ga-PET tracers and radiometal therapeutics with identical chemical structure. Co-injection allows for monitoring the in vivo

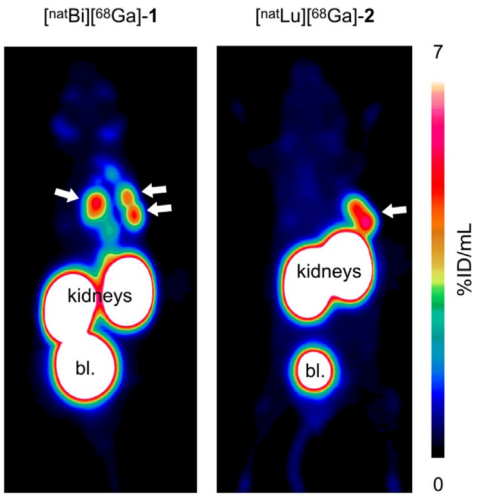

Figure 2. PET images (MIP, 60 min p.i.) of LNCaP (human prostate carcinoma) tumor bearing SCID mice, obtained with ^{68}Ga-labeled [natBi]-**1** and [natLu]-**2**, respectively. Tumor positions are indicated with white arrows. In the left image, multiple uptake foci correspond to presence of several small tumor lesions. bl. = bladder.

Table 1. In-vitro data and PET-based uptake values for [^{nat}Bi][^{68}Ga]-**1** and [^{nat}Lu][^{68}Ga]-**2** (60 min p.i., 15 min acquisition time).[a]

	[^{nat}Bi][$^{nat/68}$Ga]-**1**	[^{nat}Lu][$^{nat/68}$Ga]-**2**
IC_{50} [nM]	2.5 ± 0.2	2.8 ± 0.3
log *D*	−4.4 ± 0.1	−3.8 ± 0.1
tumor [%ID/mL]	2.8 ± 0.3	3.3 ± 0.2
kidney [%ID/mL]	21 ± 6	54 ± 10
muscle [%ID/mL]	0.13 ± 0.01	0.17 ± 0.07
salivary gland [%ID/mL]	0.57 ± 0.25	0.44 ± 0.13

[a] 50% inhibition concentrations (IC_{50}) were determined using the nonradioactive compounds.

distribution of the radiotherapeutics by PET and thus enables therapeutic dosimetry with improved precision and accelerated workflows. Although the synthetic approach allows the use of any radiolanthanide, the prerequisite of matching half-lives suggests primary use with ^{213}Bi. Notwithstanding this, the possibility of performing fast and accurate PET-based dosimetry for ^{213}Bi-labeled therapeutics might further promote ^{213}Bi-based alpha-therapy, representing a last option for cancer patients refractory to established external or internal radiation treatments.

Acknowledgements

Support by the Deutsche Forschungsgemeinschaft (grant #NO822/4-1 and CRC 824) is gratefully acknowledged. We thank Frauke Hoffmann, Martina Wirtz, Sybille Reder and Markus Mittelhäuser for assistance with cell cultures and animal experiments.

Conflict of interest

The authors declare no conflict of interest.

Keywords: chelate ligands · click chemistry · molecular imaging · molecular radiotherapy · radionuclides

[1] W. J. G. Oyen, L. Bodei, F. Giammarile, H. R. Maecke, J. Tennvall, M. Luster, B. Brans, *Ann. Oncol.* **2007**, *18*, 1782 – 1792.
[2] D. R. McGowan, M. J. Guy, *Br. J. Radiol.* **2015**, *88*, 20140720.
[3] A. Sabet, J. Nagarajah, A. S. Dogan, H.-J. Biersack, A. Sabet, S. Guhlke, S. Ezziddin, *EJNMMI Res.* **2013**, *3*, 82.
[4] I. Velikyan, A. Sundin, B. Eriksson, H. Lundqvist, J. Sörensen, M. Bergström, B. Långström, *Nucl. Med. Biol.* **2010**, *37*, 265 – 275.
[5] J. Notni, K. Steiger, F. Hoffmann, D. Reich, M. Schwaiger, H. Kessler, H. J. Wester, *J. Nucl. Med.* **2016**, *57*, 1618 – 1624.
[6] M. W. Konijnenberg, W. A. P. Breeman, E. de Blois, H. S. Chan, O. C. Boerman, P. Laverman, P. Kolenc-Peitl, M. Melis, M. de Jong, *EJNMMI Res.* **2014**, *4*, 47.
[7] V. Tolmachev, D. Rosik, H. Wållberg, A. Sjöberg, M. Sandström, M. Hansson, A. Wennborg, A. Orlova, *Eur. J. Nucl. Med. Mol. Imaging* **2010**, *37*, 613 – 622.
[8] J.-M. Beauregard, M. S. Hofman, G. Kong, R. J. Hicks, *Eur. J. Nucl. Med. Mol. Imaging* **2012**, *39*, 50 – 56.
[9] C. T. Mendler, A. Feuchtinger, I. Heid, M. Aichler, C. D'Alessandria, S. Pirsig, B. Blechert, H. J. Wester, R. Braren, A. Walch, A. Skerra, M. Schwaiger, *J. Nucl. Med.* **2016**, *57*, 1971 – 1977.
[10] H. J. Wester, U. Keller, M. Schottelius, A. Beer, K. Philipp-Abbrederis, F. Hoffmann, J. Šimeček, C. Gerngross, M. Lassmann, K. Herrmann, N. Pellegata, M. Rudelius, H. Kessler, M. Schwaiger, *Theranostics* **2015**, *5*, 618 – 630.
[11] V. Tolmachev, H. Wållberg, M. Sandström, M. Hansson, A. Wennborg, A. Orlova, *Eur. J. Nucl. Med. Mol. Imaging* **2011**, *38*, 531 – 539.
[12] B. Brans, L. Bodei, F. Giammarile, O. Linden, M. Luster, W. J. Oyen, J. Tennvall, *Eur. J. Nucl. Med. Mol. Imaging* **2007**, *34*, 772 – 786.
[13] T. Wadas, E. H. Wong, G. R. Weisman, C. J. Anderson, *Chem. Rev.* **2010**, *110*, 2858 – 2902.
[14] G. J. Stasiuk, N. J. Long, *Chem. Commun.* **2013**, *49*, 2732 – 2746.
[15] A. Morgenstern, F. Bruchertseifer, C. Apostolidis, *Curr. Radiopharm.* **2012**, *5*, 221 – 227.
[16] M. Ljungberg, A. Celler, M. W. Konijnenberg, K. F. Eckerman, Y. K. Dewaraja, K. Sjögreen-Gleisner, W. E. Bolch, A. B. Brill, F. Fahey, D. R. Fisher, R. Hobbs, R. W. Howell, R. F. Meredith, G. Sgouros, P. Zanzonico, K. Bacher, C. Chiesa, G. Flux, M. Lassmann, L. Strigari, S. Walrand, *J. Nucl. Med.* **2016**, *57*, 151 – 162.
[17] J.-M. Beauregard, M. S. Hofman, J. M. Pereira, P. Eu, R. J. Hicks, *Cancer Imaging* **2011**, *11*, 56 – 66.
[18] F. Forrer, H. Uusijärvi, C. Waldherr, M. Cremonesi, P. Bernhardt, J. Mueller-Brand, H. R. Maecke, *Eur. J. Nucl. Med. Mol. Imaging* **2004**, *31*, 1257 – 1262.
[19] G. Flux, M. Bardies, M. Monsieurs, S. Savolainen, S. E. Strand, M. Z. Lassmann, *Z. Med. Phys.* **2006**, *16*, 47 – 59.
[20] F. Rösch, H. Herzog, S. M. Qaim, *Pharmaceuticals* **2017**, *10*, 56.
[21] G. J. Förster, M. J. Engelbach, J. J. Brockmann, H. J. Reber, H. G. Buchholz, H. R. Mäcke, F. R. Rösch, H. R. Herzog, P. R. Bartenstein, *Eur. J. Nucl. Med.* **2001**, *28*, 1743 – 1750.
[22] S. Walrand, G. D. Flux, M. W. Konijnenberg, R. Valkema, E. P. Krenning, R. Lhommel, S. Pauwels, F. Jamar, *Eur. J. Nucl. Med. Mol. Imaging* **2011**, *38*, 57 – 68.
[23] F. Roesch, *Curr. Radiochem.* **2012**, *5*, 202 – 211.
[24] J. Notni, *Nachr. Chem.* **2012**, *60*, 645 – 649.
[25] F. Rösch, *Appl. Radiat. Isot.* **2013**, *76*, 24 – 30.
[26] R. P. Baum, H. R. Kulkarni, *Theranostics* **2012**, *2*, 437 – 447.
[27] C. A. Umbricht, M. Benešová, R. M. Schmid, A. Türler, R. Schibli, N. P. van der Meulen, C. Müller, *EJNMMI Res.* **2017**, *7*, 9.
[28] A. Heppeler, J. P. André, I. Buschmann, X. Wang, J.-C. Reubi, M. Hennig, T. A. Kaden, H. R. Maecke, *Chem. Eur. J.* **2008**, *14*, 3026 – 3034.
[29] J. Šimeček, P. Hermann, J. Havlíčková, E. Herdtweck, T. G. Kapp, N. Engelbogen, H. Kessler, H. J. Wester, J. Notni, *Chem. Eur. J.* **2013**, *19*, 7748 – 7757.
[30] J. Notni, J. Šimeček, H. J. Wester, *ChemMedChem* **2014**, *9*, 1107 – 1115.
[31] J. Šimeček, H. J. Wester, J. Notni, *Dalton Trans.* **2012**, *41*, 13803 – 13806.
[32] J. Šimeček, P. Hermann, H. J. Wester, J. Notni, *ChemMedChem* **2013**, *8*, 95 – 103.
[33] J. Šimeček, O. Zemek, P. Hermann, J. Notni, H. J. Wester, *Mol. Pharm.* **2014**, *11*, 3893 – 3903.
[34] J. R. Mesters, C. Barinka, W. Li, T. Tsukamoto, P. Majer, B. S. Slusher, J. Konvalinka, R. Hilgenfeld, *EMBO J.* **2006**, *25*, 1375 – 1384.
[35] D. Reich, A. Wurzer, M. Wirtz, V. Stiegler, P. Spatz, J. Pollmann, H. J. Wester, J. Notni, *Chem. Commun.* **2017**, *53*, 2586 – 2589.
[36] Z. Baranyai, D. Reich, A. Vágner, M. Weineisen, I. Tóth, H. J. Wester, J. Notni, *Dalton Trans.* **2015**, *44*, 11137 – 11146.
[37] J. Notni, H. J. Wester, *Chem. Eur. J.* **2016**, *22*, 11500 – 11508.
[38] J. Notni, P. Hermann, J. Havlíčková, J. Kotek, V. Kubíček, J. Plutnar, N. Loktionova, P. J. Riss, F. Rösch, I. Lukeš, *Chem. Eur. J.* **2010**, *16*, 7174 – 7185.
[39] J. Šimeček, M. Schulz, J. Notni, J. Plutnar, V. Kubíček, J. Havlíčková, P. Hermann, *Inorg. Chem.* **2012**, *51*, 577 – 590.
[40] J. Notni, J. Šimeček, P. Hermann, H. J. Wester, *Chem. Eur. J.* **2011**, *17*, 14718 – 14722.
[41] M. Weineisen, J. Šimeček, M. Schottelius, M. Schwaiger, H. J. Wester, *EJNMMI Res.* **2014**, *4*, 63.
[42] M. Benešová, U. Bauder-Wüst, M. Schäfer, K. D. Klika, W. Mier, U. Haberkorn, K. Kopka, M. Eder, *J. Med. Chem.* **2016**, *59*, 1761 – 1775.

Manuscript received: May 23, 2017
Accepted manuscript online: August 21, 2017
Version of record online: September 14, 2017

